Research Square

Preprints are preliminary reports that have not undergone peer review.
They should not be considered conclusive, used to inform clinical practice,
or referenced by the media as validated information.

The Signal Peptide-like Sequence SP DrwH Mediates Membrane Targeting of DrwH and Confers Heterologous Toxicity toward the Escherichia coli Cell Envelope

Ningyou Tang
Ministry of Education, Southwest University of Science and Technology
Zhiqing Liang
Ministry of Education, Southwest University of Science and Technology
Huan Yang
Ministry of Education, Southwest University of Science and Technology
Qian Fu
Ministry of Education, Southwest University of Science and Technology
Jinlong Lai
Ministry of Education, Southwest University of Science and Technology
Hanhan Li
Ministry of Education, Southwest University of Science and Technology
Yu Zhang
Ministry of Education, Southwest University of Science and Technology
Zhengfu Zhou
Chinese Academy of Agricultural Sciences
Shijie Jiang
sjjiang0406@swust.edu.cn

Ministry of Education, Southwest University of Science and Technology

Research Article

Keywords: signal peptide-like SPDrwH, DrwH protein, Escherichia coli, membrane targeting, heterologous cytotoxicity

Posted Date: November 20th, 2026

DOI: https://doi.org/10.21203/rs.3.rs-11374334/v1

License: This work is licensed under a Creative Commons Attribution 4.0 International License.
Read Full License

Additional Declarations: No competing interests reported.

Abstract

The subcellular localization of bacterial proteins depends on targeting sequences such as signal peptides. Whether signal peptide-like motifs can be recognized to exert biological functions across species remains poorly understood. Here we characterized SP_{DrwH}, an N-terminal signal peptide-like sequence of hydrophobic protein DrwH from *Deinococcus radiodurans*. Recombinant *Escherichia coli* BL21 strains producing full-length DrwH, SP_{DrwH}-deleted ΔSP mutant and their EGFP fusions were constructed for heterologous overexpression. Bioinformatic analysis predicted that conserved SP_{DrwH} folds into an amphipathic α-helix. Confocal microscopy verified that SP_{DrwH} mediates DrwH targeting to the *E. coli* cell envelope. Full-length DrwH triggered sequential outer-to-inner membrane disruption and severe host cytotoxicity, whereas the ΔSP mutant showed negligible damage phenotypes. Our results demonstrate that SP_{DrwH} acts as a functional heterologous membrane-targeting signal and confers DrwH-associated cytotoxicity toward the bacterial cell envelope. This work expands our understanding of cross-host recognition of extremophile-derived targeting elements and inspires the development of minimal synthetic-biology membrane-targeting tools. Our findings lay a solid foundation for further mechanistic investigations of signal peptide-like motifs from radiation-resistant microorganisms.

Introduction

Bacteria rely on accurate protein sorting systems to transport nascent polypeptides to specific subcellular regions. Protein subcellular localization closely correlates with biological function, and N-terminal signal peptides act as core recognition elements for protein transmembrane translocation and subcellular targeting[1]. Canonical signal peptides consist of a positively charged N-region, hydrophobic core, and peptidase cleavage site, guiding protein transmembrane transport and intracellular sorting[2]. The OmpA signal peptide of *E. coli* enables heterologous secretion of Bacillus subtilis chitosanase through the Sec pathway, and the mature protein is released into the periplasm after signal peptidase cleavage[3]. In addition to canonical signal peptides, genomic and proteomic analyses have identified non-canonical signal peptide-like sequences. These N-terminal hydrophobic sequences cannot be cleaved by signal peptidases and function in protein membrane anchoring and membrane interaction rather than conventional secretion[4]. They commonly form amphipathic α-helices that insert into lipid bilayers, stably anchoring proteins to cell membranes and regulating their biological activities[5]. In *E. coli*, MinD binds membranes reversibly via a C-terminal amphipathic helix to regulate cell division site positioning[6], while the N-terminal amphipathic helix of MinE mediates membrane association to sustain Min system oscillation[7]. Such non-canonical sequences are essential for the correct localization and function of bacterial stress proteins and membrane enzymes, which deserve further exploration.

Intact cell membranes are critical for bacterial physiological homeostasis. Heterologous proteins can disrupt membrane permeability and membrane potential via membrane binding, pore formation, or lipid disorder disruption, thereby affecting host cell survival[8, 9]. The antimicrobial peptide cecropin A inserts

into *E. coli* membranes through amphipathic α-helices to form pores, increasing dual-membrane permeability, collapsing membrane potential, and causing cell death[10]. Heterologous membrane protein overexpression often induces cytotoxicity and growth inhibition in *E. coli*, and the C41(DE3) and C43(DE3) strains were developed to tolerate such membrane protein toxicity[11]. As a mature prokaryotic heterologous expression host, *E. coli* is widely used to analyze exogenous protein localization and protein-membrane interactions for cross-species protein targeting and membrane damage research[12]. Signal peptide-mediated membrane targeting is a key cause of heterologous protein-induced membrane perturbation and cytotoxicity. However, the membrane-associated functions of extremophile-derived signal peptide-like sequences in *E. coli* remain poorly studied.

D. radiodurans is well-known for its strong resistance to extreme stresses, and its genome encodes numerous functional proteins involved in DNA repair, oxidative stress tolerance, and membrane homeostasis[13]. PprA interacts with DNA gyrase to regulate chromosome segregation and DNA damage repair[14]. DdrB mediates RecA-independent single-strand DNA annealing during DNA repair[15]. KatA eliminates intracellular reactive oxygen species to improve oxidative tolerance, and its deletion increases bacterial sensitivity to ionizing radiation[16]. Most previous studies focus on soluble intracellular proteins, while the cross-host expression characteristics and membrane interaction mechanisms of *D. radiodurans* membrane proteins remain unclear. Our preliminary study found that the hydrophobic protein DrwH encoded by *dr1372* contains an N-terminal signal peptide-like sequence SP_{DrwH}. In *E. coli*, overexpression of full-length DrwH significantly inhibits cell growth, whereas the SP_{DrwH}-deleted mutant shows no inhibitory effect. Previous studies have only explored the stress resistance of DrwH in *D. radiodurans*[17]. Whether SP_{DrwH} acts as a membrane-targeting signal to mediate DrwH localization and trigger host membrane damage remains unelucidated.

This study aimed to explore the regulatory role of SP_{DrwH} in DrwH subcellular localization and its membrane-related effects. Full-length DrwH and its SP_{DrwH}-deleted mutant were heterologously expressed in *E. coli*. Bioinformatics analysis was used to analyze SP_{DrwH} structural features. Laser confocal microscopy was applied to determine DrwH subcellular localization. Bacterial growth, cell morphology, and membrane integrity were evaluated through growth curve detection, scanning electron microscopy, flow cytometry, and inner/outer membrane permeability assays. This study clarifies the SP_{DrwH}-mediated membrane targeting mechanism of DrwH and characterizes the envelope damage associated with DrwH overexpression in *E. coli.* The findings provide fundamental data for understanding cross-host localization of extremophilic proteins and the functional mechanisms of signal peptide-like sequences.

Materials and Methods

Strains, plasmids, and culture conditions

The strains and plasmids used in this study are summarized in Table S1. *E. coli* BL21(DE3), empty vector pET28a and pET28a-EGFP were preserved in our laboratory. The recombinant plasmids pET28a-DrwH and pET28a-ΔSP were constructed in our previous work. All plasmids were transformed into competent *E. coli* BL21(DE3) cells via heat shock to generate the corresponding expression strains. Bacterial cultures were grown in LB medium at 37°C, supplemented with kanamycin at a final concentration of 50 μg/mL during cultivation.

Reagents

O-Nitrophenyl-β-D-galactopyranoside (ONPG) and propidium iodide (PI) were obtained from Fuzhou Feijing Biotechnology Co., Ltd. N-Phenyl-1-naphthylamine (NPN) was purchased from Shanghai Macklin Biochemical Co., Ltd., kanamycin and isopropyl β-D-1-thiogalactopyranoside (IPTG) were obtained from Shanghai Sangon Biotech Co., Ltd.

Construction of plasmids and recombinant strains

Genomic DNA of *D. radiodurans* served as the template. The *drwH* fragment was amplified with primer pair P1/P2, while the *egfp* fragment was amplified from plasmid pET28a-EGFP using primers P3/P4. The *drwH-egfp* fusion fragment was generated by overlap PCR using the two PCR amplicons. The fused DNA product was then inserted into the *Eco*R Ⅰ- and *Bam*H Ⅰ-digested, purified linearized pET28a vector using the ClonExpress II One-Step Cloning Kit (Vazyme Biotech Co., Ltd, Nanjing, China), generating recombinant plasmid pET28a-DrwH-EGFP. The plasmid was transformed into competent *E. coli* BL21(DE3) cells, and positive clones were verified by colony PCR and DNA sequencing. For construction of pET28a-ΔSP-EGFP, plasmid pET28a-DrwH-EGFP was used as the template. Primer pair P5/P6 was used to amplify the ΔSP-EGFP fragment. The purified PCR product was cloned into *Eco*R Ⅰ- and *Bam*H Ⅰ-double-digested linearized pET28a with the ClonExpress II One-Step Cloning Kit, yielding recombinant plasmid pET28a-ΔSP-EGFP. All primer sequences employed in the above PCR amplifications are provided in Table S2.

Bioinformatics analysis

Protein topological features were predicted using DeepTMHMM 1.0 (https://services.healthtech.dtu.dk/services/DeepTMHMM-1.0/). HeliQuest was applied to characterize the physicochemical properties and generate helical schematics of the target peptide (https://heliquest.ipmc.cnrs.fr/). Multiple-sequence alignment of homologous proteins was performed with Clustal Omega (https://www.ebi.ac.uk/Tools/msa/clustalo/) .

Laser confocal microscopy fluorescence observation

Recombinant strains BL21/EGFP, BL21/DrwH-EGFP, and the control BL21/28a were separately cultured in 10 mL LB medium supplemented with 50 μg/mL kanamycin in a constant-temperature shaker at 37°C and 200 rpm for 12 h to prepare seed cultures of recombinant *E. coli*. Each seed culture was inoculated into 20 mL LB medium containing 50 μg/mL kanamycin to reach an initial OD_{600} of 0.1, followed by incubation at 37°C with shaking at 200 rpm for 1 h until cells entered the logarithmic phase. IPTG was then added to a final concentration of 0.1 mM to induce target protein expression. Bacterial samples were harvested after induction, centrifuged at 8,000 rpm for 5 min, and the supernatant was discarded. The cell pellet was washed three times with PBS buffer, and the OD_{600} of all samples was normalized to 0.5. Subcellular localization of the target protein was visualized using a laser scanning confocal microscope with a 488 nm excitation laser; fluorescent signals within bacterial cells were captured and documented. This sample preparation protocol was also applied for subsequent scanning electron microscopy, flow cytometry, and membrane permeability assays.

Determination of growth curve

A single colony was picked from kanamycin-containing agar medium and cultured in LB liquid medium to logarithmic phase. The seed culture was inoculated into 20 mL LB medium supplemented with 50 μg/mL kanamycin to achieve an initial OD_{600} of 0.1. After 1 h incubation, 0.1 mM IPTG was added for protein induction. During cultivation, samples were collected every 2 h, and OD_{600} values were determined using a microplate reader. The empty vector strain BL21/28a was used as the control. All cultures were incubated at 37°C with shaking at 200 rpm.

Morphological observation by SEM

Scanning electron microscopy (SEM) was used to examine the surface morphological features of key recombinant strains BL21/28a, BL21/DrwH, and BL21/ΔSP after IPTG induction. Bacterial samples were harvested at four time points (0, 4, 8, and 12 h) post-induction. Bacterial suspensions were prepared as described above, followed by fixation with 2.5% glutaraldehyde. Samples were gently mixed and kept overnight at 4°C for fixation. After three washes with sterile ddH_2O, cells were subjected to a graded ethanol dehydration series (30%, 50%, 70%, 85%, 90%, and 100%), with each concentration applied for 10 min. Cells were pelleted by centrifugation at 8,000 rpm for 5 min, and the supernatant was removed. The processed samples were carefully dropped onto clean cover slips and air-dried at room temperature in a clean environment. After gold sputter coating, specimens were imaged under the scanning electron microscope. Micrographs were acquired at 10,000× magnification to evaluate bacterial population distribution and cellular morphology for subsequent analysis.

Membrane permeability determined by flow cytometry

Flow cytometry was used to assess membrane integrity of recombinant *E. coli* strains BL21/DrwH, BL21/ΔSP, and BL21/28a. Samples were harvested at four time points (0, 4, 8, and 12 h) post-induction.

Bacterial suspensions were prepared as described above, and 0.85% NaCl solution served as the blank control. For staining, propidium iodide (PI; 1 mg/mL stock) was added to the bacterial samples to a final concentration of 2 μg/mL, followed by incubation for 30 min at 4°C in the dark. After staining, the bacterial suspension was filtered through a 200-mesh cell strainer. A total of 20,000 events were acquired at a low flow rate on the flow cytometer with 488 nm excitation. The percentage of PI-positive cells was quantified to evaluate bacterial viability and mortality across groups.

Determination of outer membrane permeability using the NPN assay

A 20 μL volume of 1 mM NPN stock solution was rapidly added to the prepared bacterial suspension, and the mixture was transferred into wells of a black 96-well microplate. Fluorescence was measured using a microplate reader with excitation at 350 nm and emission at 429 nm. The final fluorescence intensity was recorded after the signal reached a stable plateau. A 0.85% NaCl solution was used for instrument blank calibration.

Determination of inner membrane permeability using the ONPG assay

Bacterial suspensions and 25 mM ONPG stock solution were pre-warmed at 37°C for 5 min. A 1 mL volume of preheated bacterial suspension adjusted to an OD_{600} of 0.5 was mixed with 60 μL of 25 mM ONPG stock solution to yield a final ONPG concentration of 1.5 mM. The mixture was thoroughly vortexed and incubated at 37°C for 30 min. The absorbance of each sample was then measured at 405 nm.

Results

Bioinformatic analysis of DrwH and signal peptide-like sequence SP_{DrwH}

Bioinformatic predictions were performed on the N-terminal 19 amino acids of DrwH, designated SP_{DrwH}. DeepTMHMM posterior probability analysis revealed a high-probability N-terminal signal peptide region in DrwH, with no predicted transmembrane helices. The rest of the protein sequence was assigned to the extramembrane region, consistent with a globular protein containing an N-terminal signal peptide (Fig. 1A). The HeliQuest helical wheel plot shows the spatial distribution of amino acid residues, with non-polar hydrophobic residues concentrate on one face of the helix, whereas charged and polar residues cluster on the opposite face, forming a canonical amphipathic α-helix (Fig. 1B). Multiple sequence alignment demonstrated that this N-terminal peptide harbours a conserved hydrophobic motif present in DrwH homologs from diverse radiation-resistant extremophiles (Fig. 1C).

Subcellular localization of DrwH in E. coli

To characterize the subcellular localization of DrwH in *E. coli*, we constructed the recombinant strain BL21/DrwH-EGFP, which produces the DrwH-EGFP fusion protein. BL21/EGFP was used as the positive control, BL21/28a as the negative control, and BL21/ΔSP-EGFP as the signal peptide deletion mutant control. Laser scanning confocal microscopy (excitation at 488 nm) of these strains showed no detectable fluorescence in the negative control BL21/28a. The positive control BL21/EGFP displayed uniform cytoplasmic green fluorescence. The ΔSP mutant strain BL21/ΔSP-EGFP exhibited diffuse intracellular green fluorescence, while BL21/DrwH-EGFP showed non-uniform fluorescent signals concentrated at the cell periphery. In addition, some BL21/DrwH-EGFP cells displayed morphological alterations with irregular cellular contours.

Overexpression of DrwH inhibits growth and alters cellular morphology in *E. coli*

Growth curves of recombinant *E. coli* strains BL21/DrwH, BL21/ΔSP, and BL21/28a were determined to assess the effect of SP_{DrwH} on bacterial growth (Fig. 3). Upon IPTG induction, BL21/DrwH expressing full-length DrwH exhibited severe growth arrest. BL21/ΔSP rapidly entered exponential phase, with higher growth rate and final biomass than the control BL21/28a, which entered stationary phase early and maintained low fluctuating cell density. BL21/DrwH showed only a transient slight increase in cell density after induction, followed by complete growth cessation. These results demonstrate that DrwH exerts strong growth-suppressive effects under heterologous overexpression and this heterologous cytotoxicity strictly depends on the presence of N-terminal SP_{DrwH}. Deletion of SP_{DrwH} completely abolished growth-inhibitory phenotypes and the ΔSP mutant exhibited superior growth compared with the control. Thus SP_{DrwH}-directed membrane targeting is indispensable for DrwH-mediated growth inhibition under heterologous overexpression. Loss of this targeting peptide eliminates cytotoxicity, indicating that DrwH-triggered cell-envelope perturbation relies on SP_{DrwH}-dependent membrane association.

Parallel to the growth curve assay, the cellular morphology of strains BL21/DrwH, BL21/ΔSP, and BL21/28a was characterized by scanning electron microscopy (SEM), revealing marked differences in cell shape, surface smoothness and envelope integrity (Fig. 4). At all time points, empty vector control BL21/28a displayed typical rod-shaped *E. coli* with smooth, intact cell surfaces, clear cell wall contours and blunt rounded poles; no obvious morphological defects were observed. At 0 h post-induction, BL21/DrwH was morphologically indistinguishable from the control, retaining regular rod morphology and smooth surfaces. With prolonged induction (4 h), partial cells developed mild surface wrinkling and local indentations. By 8 h, wrinkling and surface roughness were aggravated, accompanied by cell twisting, envelope damage and altered aspect ratios. At 12 h, most BL21/DrwH cells showed severe dehydration, extensive surface folding, local rupture and cytoplasmic leakage; prominent cell aggregation and cellular debris were also visible. In contrast, BL21/ΔSP maintained smooth, intact rod morphology at all time points without obvious shrinkage or damage. These results demonstrate that the N-terminal SP_{DrwH} is required for morphological defects and cell-envelope damage observed under

heterologous overexpression. SP_{DrwH} mediates membrane targeting of DrwH toward the bacterial cell envelope and this localization event serves as a prerequisite for subsequent heterologous cytotoxicity and growth suppression.

Signal peptide-like peptide SP_{DrwH} impairs cell membrane integrity

Flow cytometry with propidium iodide (PI) staining was applied to quantify cell death across strains over the induction time course (Fig. 5). The PI-positive ratio of empty-vector control BL21/28a remained relatively stable: 35.05% at 0 h, slightly increasing to 36.38% at 4 h and 46.51% at 8 h before dropping to 16.01% at 12 h. This suggests that IPTG and the empty plasmid exerted only mild baseline toxicity, with no large fluctuations in cell death. The BL21/ΔSP displayed significantly lower PI-positive percentages at all time points (26.17% at 0 h, 13.03% at 4 h, 12.83% at 8 h, and 14.56% at 12 h), indicating that removal of SP_{DrwH} alleviated the toxicity caused by recombinant protein expression. In contrast, BL21/DrwH showed a distinct trend. Its PI-positive rate was 16.19% at 0 h (comparable to BL21/ΔSP), but rapidly increased to 44.76% at 4 h, peaked at 80.65% at 8 h, and stayed at 75.49% at 12 h. During 8–12 h post-induction, its PI-positive proportion was approximately 1.6–5.0-fold higher than the control. These results quantitatively verify the heterologous cytotoxicity triggered by DrwH under heterologous overexpression and confirm such lethal phenotypes are strictly dependent on the signal peptide-like sequence SP_{DrwH}.

To further dissect how SP_{DrwH} modulates the membrane permeability of *E. coli* BL21, outer membrane (OM) and inner membrane (IM) permeability were assessed separately. As shown in Fig. 6A, the outer membrane permeability of *E. coli* BL21 increased in a time-dependent manner. At 0 h post-induction, all three strains exhibited low and comparable baseline NPN fluorescence, indicating intact outer membranes with no intergroup differences. During induction, NPN fluorescence of BL21/28a remained low without obvious elevation, demonstrating that empty vector expression barely altered outer membrane permeability. For BL21/DrwH, NPN fluorescence rose significantly starting at 4 h post-induction and peaked at 12 h, values were markedly higher than the control at matched time points, showing that DrwH expression progressively increases outer membrane permeability and impairs barrier function. Although BL21/ΔSP displayed marginally higher NPN fluorescence than BL21/28a at all time points, its signal was substantially lower than BL21/DrwH with a much slower rising rate. These permeability data verify that the N-terminal SP_{DrwH} is the key domain responsible for DrwH-mediated outer membrane damage. This signal peptide-like sequence targets DrwH to the outer membrane and disrupts its barrier integrity, allowing massive entry of the hydrophobic probe NPN, which provides direct evidence for the membrane-permeabilizing toxicity of DrwH. Inner membrane permeability, measured by OD_{405} (Fig. 6B), showed low and comparable initial values across all groups, reflecting intact inner membranes at induction onset. With prolonged induction, OD_{405} of BL21/28a slightly increased then plateaued. BL21/DrwH exhibited elevated OD_{405} after induction and maintained higher values than the

control, revealing that DrwH expression increases inner membrane permeability. By contrast, BL21/ΔSP had OD_{405} values similar to or slightly lower than the control and remained stable over time, suggesting that removal of the N-terminal signal peptide preserves inner membrane stability. Collectively, these findings indicate that SP_{DrwH}-mediated membrane targeting is required for outer-membrane disruption, while accumulation of full-length DrwH further contributes to inner-membrane injury. Deletion of SP_{DrwH} largely relieves membrane permeabilization and maintains cell-envelope homeostasis in the heterologous host.

Discussion

The accurate subcellular localization of proteins is essential for microbial biological functions, and N-terminal targeting sequences serve as core regulators of intracellular trafficking, membrane anchoring and membrane interactions[18]. Unlike well-studied canonical signal peptides, signal peptide-like motifs remain poorly characterized with respect to cross-species recognition and downstream biological outcomes[19–21]. In this work, we focused on SP_{DrwH}, an N-terminal signal peptide-like motif from radiation-resistant *D. radiodurans*. Our heterologous expression assays demonstrate that SP_{DrwH} mediates membrane targeting of DrwH and is essential for the heterologous cytotoxicity exerted against the *E. coli* cell envelope. SP_{DrwH} is an 19-residue peptide enriched in positively charged residues at its N-terminus and contains a hydrophobic stretch that forms a typical amphipathic α-helix. These structural characteristics are comparable to well-characterized bacterial membrane-anchoring proteins including FtsA and MinE[22, 23]. Its comparatively short hydrophobic core may enable functional compensation via electrostatic interactions between the peptide's positively charged residues and negatively charged phospholipid head-groups of bacterial membranes. SP_{DrwH} lacks identifiable signal peptidase cleavage sites, which supports its classification as a non-cleavable signal peptide-like anchor. Truncation mutagenesis suggests that deletion of SP_{DrwH} abolishes membrane association and sequesters DrwH within the cytoplasm. In contrast to virulence-related toxic proteins derived from pathogenic bacteria such as PlaS[24], SP_{DrwH} exhibits a minimal sequence architecture, and its native origin from non-pathogenic Deinococcus also confers favorable biosafety attributes relative to pathogen-derived toxins for prospective synthetic-biology applications.

Confocal microscopy observations provide visual evidence confirming the cross-species membrane-targeting function of SP_{DrwH} in *E. coli*. The DrwH-EGFP fusion carrying intact SP_{DrwH} accumulates primarily at the cell periphery and division septa, whereas the ΔSP-EGFP mutant displays diffuse cytoplasmic distribution with no obvious membrane enrichment. These findings suggest that this non-canonical signal peptide can be recognized and utilized as a membrane anchor within heterologous bacterial hosts. Such amphipathic-helix-dependent membrane anchoring is evolutionarily conserved among prokaryotes; many bacterial membrane-associated proteins rely on N- or C-terminal hydrophobic helices for membrane binding[6, 22]. The present study further illustrates that extremophile-derived non-canonical signal peptides can cross species barriers to achieve precise membrane targeting in *E. coli*, adding new evidence for understanding cross-host recognition of signal peptide-like sequences.

SP_{DrwH}-dependent membrane localization appears to trigger progressive structural damage of the *E. coli* cell envelope and disrupt normal cellular morphology. SEM ultrastructural observations reveal time-dependent damage in strains expressing full-length DrwH. With prolonged induction, cells gradually transition from smooth intact rod-shaped morphology to wrinkled surfaces with indentations and protruding membrane vesicles, ultimately leading to cell distortion, lysis and leakage of intracellular contents. The ΔSP mutant retains intact cellular morphology without obvious damage phenotypes, indicating that mature DrwH alone does not exert membrane toxicity and that cytotoxicity requires SP_{DrwH}-mediated membrane association. This progressive damage pattern resembles the toxicity induced by heterologous expression of PlaS from *Serratia marcescens*, where membrane disruption is initiated by an N-terminal hydrophobic targeting sequence[25]. Growth curve results further support these morphological observations; full-length DrwH expression strongly suppresses host proliferation, while SP_{DrwH} deletion relieves protein toxicity and restores normal bacterial growth. It should be noted, however, that these data establish SP_{DrwH} as a required anchoring element for DrwH-mediated envelope toxicity, rather than demonstrating that the isolated SP_{DrwH} peptide itself acts as a standalone membrane-disrupting agent. Whether the free peptide alone is sufficient to perturb membranes, or whether it acts in concert with the mature DrwH moiety, remains to be determined by independent expression of the isolated peptide.

Membrane permeability assays and flow cytometry quantitatively characterize the sequential outer-to-inner membrane damage and lethal effects associated with SP_{DrwH}-dependent membrane localization of DrwH. NPN and ONPG assays demonstrate that DrwH first impairs outer-membrane barrier properties before disrupting inner-membrane integrity, indicating a stepwise mode of envelope attack. PI staining confirms severe cell death in the strain expressing intact DrwH, while the SP_{DrwH}-truncated mutant maintains low mortality. This stepwise bilayer disruption shares similarities with the mode of action of amphipathic antimicrobial peptides such as NK-18[26]. Collectively, these observations directly link SP_{DrwH}-mediated membrane anchoring to loss of membrane integrity and cell death, and they support a model in which membrane-associated DrwH progressively compromises the permeability barrier of the *E. coli* envelope.

The divergent physiological effects of DrwH observed between its native host and *E. coli* highlight functional differences accompanying cross-host expression of extremophile proteins, which may arise from host-specific expression control and membrane microenvironmental variation. In *D. radiodurans*, endogenous DrwH is presumed to participate in cell-membrane homeostasis and stress tolerance under tightly regulated low-level expression[17]. However, T7-driven overexpression in *E. coli* leads to massive DrwH accumulation at the cell envelope, exceeding membrane tolerance and disturbing lipid organization. Previous reports indicate that high-level heterologous expression of membrane proteins can saturate the SRP-dependent Sec translocation pathway. Extremophile-origin proteins may also be poorly handled by host chaperone systems, leading to misfolding, aberrant membrane insertion and cytotoxicity[27, 28]. The cytoplasmic chaperones and the SRP-Sec targeting and translocation machinery of *E. coli* exhibit low recognition efficiency for substrates from evolutionarily distant extremophiles such

as *Deinococcus*. Limited chaperone assistance and saturated transport pathways may allow disordered insertion of DrwH into lipid bilayers and exacerbate membrane damage. These considerations provide a plausible mechanistic explanation for the cross-host functional divergence of DrwH observed in the present study, although direct measurements of native DrwH expression levels and chaperone engagement will be required to substantiate this model.

This study identifies dual roles for SP_{DrwH}, acting both as a membrane-targeting element and as a contributor to envelope perturbation in *E. coli*. The present findings expand the mechanistic framework of non-canonical signal peptides, which are not limited solely to protein transport. Consistent with earlier studies, cation-rich short amphipathic α-helices can bind lipid bilayers via electrostatic compensation for weak hydrophobic anchoring and alter lipid packing; their surface charge modulates membrane disruption severity[29]. In Gram-negative bacteria, such cationic helices preferentially bind outer-membrane lipopolysaccharides and initiate sequential outer-to-inner bilayer injury, producing morphological changes including membrane vesicle formation[30]. Helical fragments capable of LPS binding can permeabilize Gram-negative membranes and act as antibiotic-sensitizing moieties, and peptide activity can be tuned through sequence modification[31]. Amphipathic helical sequences from non-pathogenic microbes also offer biosafety advantages for antimicrobial development compared with virulence proteins from pathogens[32]. SP_{DrwH}'s compact structure, origin from a non-pathogenic organism and ease of synthesis make it a promising candidate for synthetic-biology exploitation, although its intrinsic cytotoxicity toward *E. coli* must be taken into account in engineering applications. Further investigations, including independent expression of the isolated SP_{DrwH} peptide, will help distinguish between the two mechanistic possibilities and clarify the molecular basis of membrane perturbation. Additional work is also needed to explore the native physiological roles of SP_{DrwH} in *D. radiodurans*, its antimicrobial spectrum against drug-resistant pathogens, and the key residues responsible for membrane binding and bilayer disruption.

Conclusion

This study characterizes SPDrwH, an N-terminal signal peptide-like sequence of DrwH from *D. radiodurans*. Bioinformatic predictions and fluorescence localization assays show that SP_{DrwH} mediates the anchoring of heterologously expressed full-length DrwH to the *E. coli* cell envelope. Results from scanning electron microscopy, membrane permeability assays and flow cytometry reveal that SP_{DrwH}-dependent membrane targeting is required for DrwH-associated cytotoxicity, cell-envelope damage and bacterial growth inhibition. The ΔSP mutant lacking SP_{DrwH} retains intact cell-envelope integrity and exhibits phenotypes comparable to the empty vector control. Our findings identify SP_{DrwH} as a compact membrane-targeting element for heterologous protein delivery.

Declarations

Supplementary Information

The online version contains supplementary material available at XXX

Competing interests

The authors declare no competing interests.

Funding

This work was supported by the Third Xinjiang Scientific Expedition (2022xjkk020602) and 2026 National Training Program of Innovation for Undergraduates (S202610619014).

Author Contribution

Ningyou Tang: Investigation, Methodology, Data curation, Validation, Visualization, Writing-original draft. Zhiqing Liang: Methodology, Data curation, Validation, Formal analysis, Visualization. Huan Yang: Methodology, Validation, Formal analysis. Qian Fu: Supervision, Project administration. Jinlong Lai: Supervision, Formal analysis. Hanhan Li: Methodology, Visualization. Yu Zhang: Conceptualization, Project administration. Zhengfu Zhou: Conceptualization, Funding acquisition, Writing-review and editing. Shijie Jiang: Conceptualization, Funding acquisition, Project administration, Resources, Supervision, Writing-review and editing.

Acknowledgement

We appreciate Scientific Compass for laser scanning confocal microscopy technical support, and the Analysis and Testing Center of Southwest University of Science and Technology for scanning electron microscopy assistance. We thank laboratory colleagues for valuable discussions.

Data Availability

All the data are submitted in the manuscript.

References

1. Carlsson F, Stålhammar-Carlemalm M, Flärdh K, Sandin C, Carlemalm E, Lindahl G (2006) Signal sequence directs localized secretion of bacterial surface proteins. Nature 442(7105):943–946. https://doi.org/10.1038/nature05021
2. Tjalsma H, Bolhuis A, Jongbloed JD, Bron S, van Dijl JM (2000) Signal peptide-dependent protein transport in Bacillus subtilis: a genome-based survey of the secretome. Microbiol Mol biology reviews: MMBR 64(3):515–547. https://doi.org/10.1128/MMBR.64.3.515-547.2000

3. Pechsrichuang P, Songsiriritthigul C, Haltrich D, Roytrakul S, Namvijtr P, Bonaparte N, Yamabhai M (2016) OmpA signal peptide leads to heterogenous secretion of B. subtilis chitosanase enzyme from E. coli expression system. SpringerPlus 5(1):1200. https://doi.org/10.1186/s40064-016-2893-y
4. Bruno Martoglio; Bernhard Dobberstein (1998) Signal sequences: more than just greasy peptides. 8(10):410–415. https://doi:10.1016/s0962-8924(98)01360-9
5. Tamm LK, Tomich JM, Saier MH Jr (1989) Membrane incorporation and induction of secondary structure of synthetic peptides corresponding to the N-terminal signal sequences of the glucitol and mannitol permeases of Escherichia coli. J Biol Chem 264(5):2587–2592
6. Zhou H, Lutkenhaus J (2003) Membrane binding by MinD involves insertion of hydrophobic residues within the C-terminal amphipathic helix into the bilayer. J Bacteriol 185(15):4326–4335. https://doi.org/10.1128/JB.185.15.4326-4335.2003
7. Shih YL, Le T, Rothfield L (2003) Division site selection in Escherichia coli involves dynamic redistribution of Min proteins within coiled structures that extend between the two cell poles. Proc Natl Acad Sci USA 100(13):7865–7870. https://doi.org/10.1073/pnas.1232225100
8. Silhavy TJ, Kahne D, Walker S (2010) The bacterial cell envelope. Cold Spring Harb Perspect Biol 2(5):a000414. https://doi.org/10.1101/cshperspect.a000414
9. Narayanan A, Ridilla M, Yernool DA (2011) Restrained expression, a method to overproduce toxic membrane proteins by exploiting operator-repressor interactions. Protein science: publication Protein Soc 20(1):51–61. https://doi.org/10.1002/pro.535
10. Rangarajan N, Bakshi S, Weisshaar JC, Biochemistry (2013) 52(38), 6584–6594. https://doi.org/10.1021/bi400785j
11. Miroux B, Walker JE (1996) Over-production of proteins in Escherichia coli: mutant hosts that allow synthesis of some membrane proteins and globular proteins at high levels. J Mol Biol 260(3):289–298. https://doi.org/10.1006/jmbi.1996.0399
12. Jamin N, Garrigos M, Jaxel C, Frelet-Barrand A, Orlowski S (2018) Ectopic Neo-Formed Intracellular Membranes in Escherichia coli: A Response to Membrane Protein-Induced Stress Involving Membrane Curvature and Domains. Biomolecules 8(3):88. https://doi.org/10.3390/biom8030088
13. Chen Z, Tang Y, Hua Y, Zhao Y (2020) Structural features and functional implications of proteins enabling the robustness of Deinococcus radiodurans. Comput Struct Biotechnol J 18:2810–2817. https://doi.org/10.1016/j.csbj.2020.09.036
14. Devigne A, Guérin P, Lisboa J, Quevillon-Cheruel S, Armengaud J, Sommer S, de la Bouthier C, Servant P (2016) PprA Protein Is Involved in Chromosome Segregation via Its Physical and Functional Interaction with DNA Gyrase in Irradiated Deinococcus radiodurans Bacteria. mSphere 1(1):e00036–e00015. https://doi.org/10.1128/mSphere.00036-15
15. Xu G, Lu H, Wang L, Chen H, Xu Z, Hu Y, Tian B, Hua Y (2010) DdrB stimulates single-stranded DNA annealing and facilitates RecA-independent DNA repair in Deinococcus radiodurans. DNA Repair 9(7):805–812. https://doi.org/10.1016/j.dnarep.2010.04.006

16. Markillie LM, Varnum SM, Hradecky P, Wong KK (1999) Targeted mutagenesis by duplication insertion in the radioresistant bacterium Deinococcus radiodurans: radiation sensitivities of catalase (katA) and superoxide dismutase (sodA) mutants. J Bacteriol 181(2):666–669. https://doi.org/10.1128/JB.181.2.666-669.1999
17. Jiang S, Wang J, Liu X, Liu Y, Guo C, Zhang L, Han J, Wu X, Xue D, Gomaa AE, Feng S, Zhang H, Chen Y, Ping S, Chen M, Zhang W, Li L, Zhou Z, Zuo K, Li X, Yang Y, Lin M (2017) DrwH, a novel WHy domain-containing hydrophobic LEA5C protein from Deinococcus radiodurans, protects enzymatic activity under oxidative stress. Sci Rep 7(1):9281. https://doi.org/10.1038/s41598-017-09541-2
18. Kaushik S, He H, Dalbey RE (2022) Bacterial Signal Peptides- Navigating the Journey of Proteins. Front Physiol 13:933153. https://doi:10.3389/fphys.2022.933153
19. Bendtsen JD, Kiemer L, Fausbøll A, Brunak S (2005) Non-classical protein secretion in bacteria. BMC Microbiol 5:58. https://doi.org/10.1186/1471-2180-5-58
20. Payne SH, Bonissone S, Wu S, Brown RN, Ivankov DN, Frishman DPaša-Tolić L, Smith RD, Pevzner PA (2012) Unexpected Diversity of Signal Peptides in Prokaryotes. https://doi.org/10.1128/mbio.00339-12. mBio3:10.1128/mbio.00339 – 12
21. Fekkes P, Driessen AJ (1999) Protein targeting to the bacterial cytoplasmic membrane. Microbiol Mol biology reviews: MMBR 63(1):161–173. https://doi.org/10.1128/MMBR.63.1.161-173.1999
22. Pichoff S, Lutkenhaus J (2005) Tethering the Z ring to the membrane through a conserved membrane targeting sequence in FtsA. Mol Microbiol 55(6):1722–1734. https://doi.org/10.1111/j.1365-2958.2005.04522.x
23. Shih YL, Huang KF, Lai HM, Liao JH, Lee CS, Chang CM, Mak HM, Hsieh CW, Lin CC (2011) The N-terminal amphipathic helix of the topological specificity factor MinE is associated with shaping membrane curvature. PLoS ONE 6(6):e21425. https://doi.org/10.1371/journal.pone.0021425
24. Li X, Zhou J, Han R, Yu F, Liu K, Zhao M, Liu Y, Xue Z, Zhao S (2023) Phosphatase A1 accessory protein PlaS from Serratia marcescens controls cell membrane permeability, fluidity, hydrophobicity, and fatty acid composition in Escherichia coli BL21. Int J Biol Macromol 253(Pt 3):126776. https://doi.org/10.1016/j.ijbiomac.2023.126776
25. Hu M, Liu J, Gan Y, Zhu H, Han R, Liu K, Liu Y, Zhao M, Li X, Xue Z (2024) N-terminal truncated phospholipase A1 accessory protein PlaS from Serratia marcescens alleviates inhibitory on host cell growth and enhances PlaA1 enzymatic activity. Bioresources Bioprocess 11(1):61. https://doi.org/10.1186/s40643-024-00777-1
26. Yan J, Wang K, Dang W, Chen R, Xie J, Zhang B, Song J, Wang R (2013) Two hits are better than one: membrane-active and DNA binding-related double-action mechanism of NK-18, a novel antimicrobial peptide derived from mammalian NK-lysin. Antimicrob Agents Chemother 57(1):220–228. https://doi.org/10.1128/AAC.01619-12
27. Snoeck S, Guidi C, De Mey M (2024) Metabolic burden explained: stress symptoms and its related responses induced by (over)expression of (heterologous) proteins in Escherichia coli. Microb Cell Fact 23(1):96. https://doi.org/10.1186/s12934-024-02370-9

28. Kruglikov A, Wei Y, Xia X (2022) Proteins from Thermophilic Thermus thermophilus Often Do Not Fold Correctly in a Mesophilic Expression System Such as Escherichia coli. ACS omega 7(42):37797–37806. https://doi.org/10.1021/acsomega.2c04786
29. Yamaguchi K, Kusumoto T, Araki T, Gomibuchi Y, Yasunaga T, Osada S, Taira J (2025) Effect of Introducing Leucine Residues into 2-Aminoisobutyric Acid-Based Amphiphilic Helical Peptides on Intermolecular Interactions and Peptide Self-Assembly. ACS omega 10(21):22184–22190. https://doi.org/10.1021/acsomega.5c02490
30. Farfán-García AE, Hernández-Peñaranda IP, Gómez-Duarte OG, Rincón-Barón EJ, Torres-Rodríguez GA, Flórez-Castillo JM (2025) Structural and functional analysis of Escherichia coli membrane disruption by Ib-M peptides. PLoS ONE 20(10):e0334029. https://doi.org/10.1371/journal.pone.0334029
31. Johnson TS, Deber CM (2025) Membrane-Active Peptides Derived from Natural Transmembrane Domains Function as Antibiotic Potentiators. ACS omega 10(17):17727–17734. https://doi.org/10.1021/acsomega.5c00109
32. Liang Y, Zhang Y, Huang Y, Xu C, Chen J, Zhang X, Huang B, Gan Z, Dong X, Huang S, Li C, Jia S, Zhang P, Yuan Y, Zhang H, Wang Y, Yuan B, Bao Y, Xiao S, Xiong M (2024) Helicity-directed recognition of bacterial phospholipid via radially amphiphilic antimicrobial peptides. Sci Adv 10(35):eadn9435. https://doi.org/10.1126/sciadv.adn9435

Figures

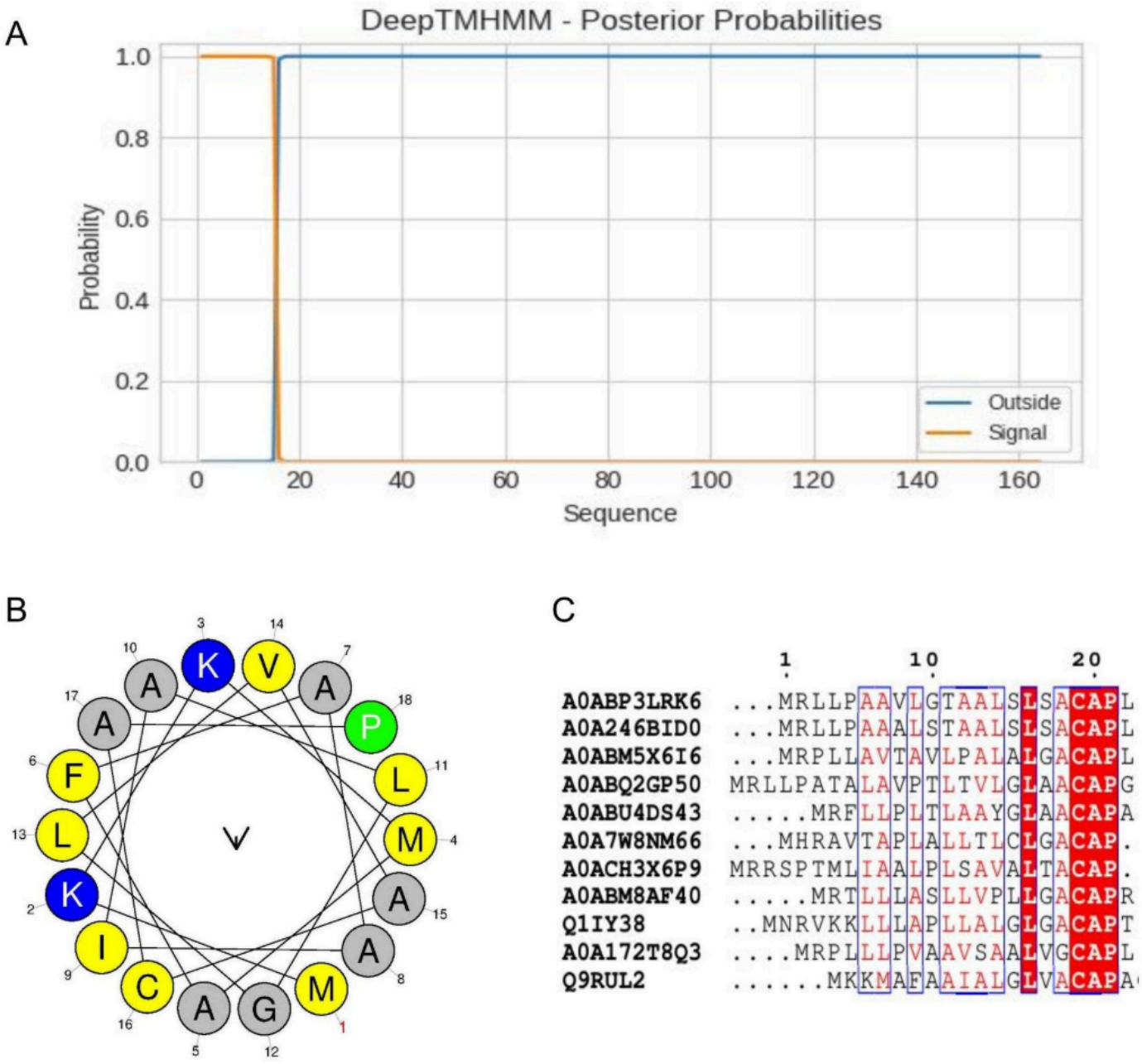


Figure 1

Prediction and bioinformatic analysis of the signal peptide-like sequence SP_{DrwH} of DrwH. (**A**) DeepTMHMM probability profile of full-length DrwH. The horizontal axis shows amino acid residue positions along the polypeptide, and the vertical axis indicates prediction probability. The orange curve represents the probability of the N-terminal signal peptide region, while the blue curve denotes the probability that residues reside on the extracellular/periplasmic side of the membrane. This profile shows the position range and prediction confidence of the putative signal peptide domain. (**B**) Helical wheel projection of the predicted amphipathic α-helix in the N-terminal SP_{DrwH}. This plot visualizes the spatial arrangement of hydrophobic, polar, positively and negatively charged amino acid residues around the helical backbone, demonstrating the amphipathic nature of this helical segment. (**C**) Multiple

sequence alignment of SP_{DrwH} and its homologous sequences from related bacterial species. Highly conserved amino acid residues are shaded in red, and solid rectangular boxes highlight the conserved motif in the aligned sequences. The sequence conservation among homologs indicates functionally critical sites within this N-terminal signal peptide-like segment.

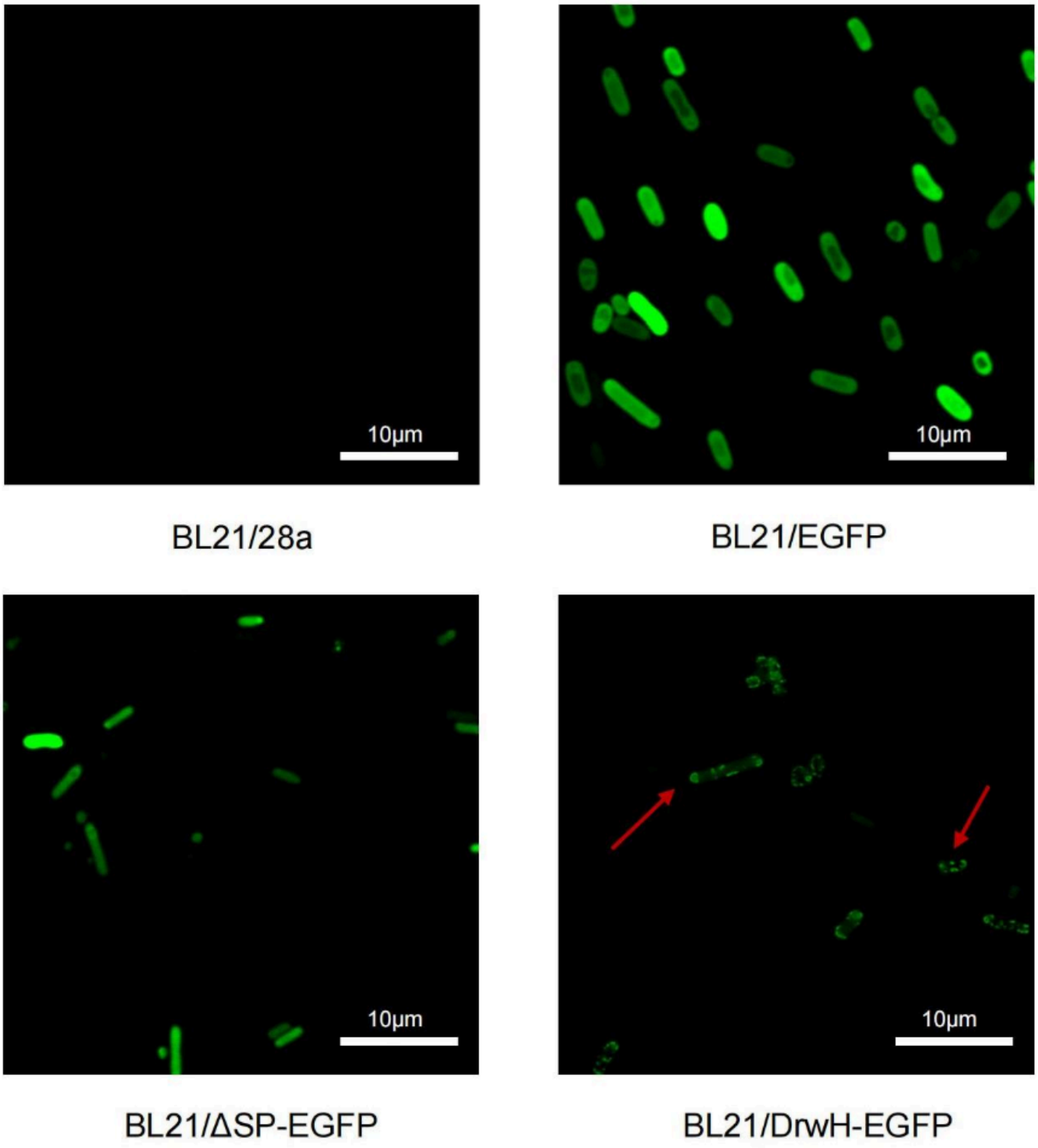


Figure 2

Subcellular localisation of fusion proteins in different recombinant strains observed by laser scanning confocal microscopy. *E. coli* BL21(DE3) strains harbouring the indicated plasmids were cultured and induced for fusion protein expression. Cell pellets were harvested, washed with sterile PBS, and subjected to confocal imaging at a third-party testing facility. Micrographs were captured with 488 nm excitation. Scale bars, 10 μm.

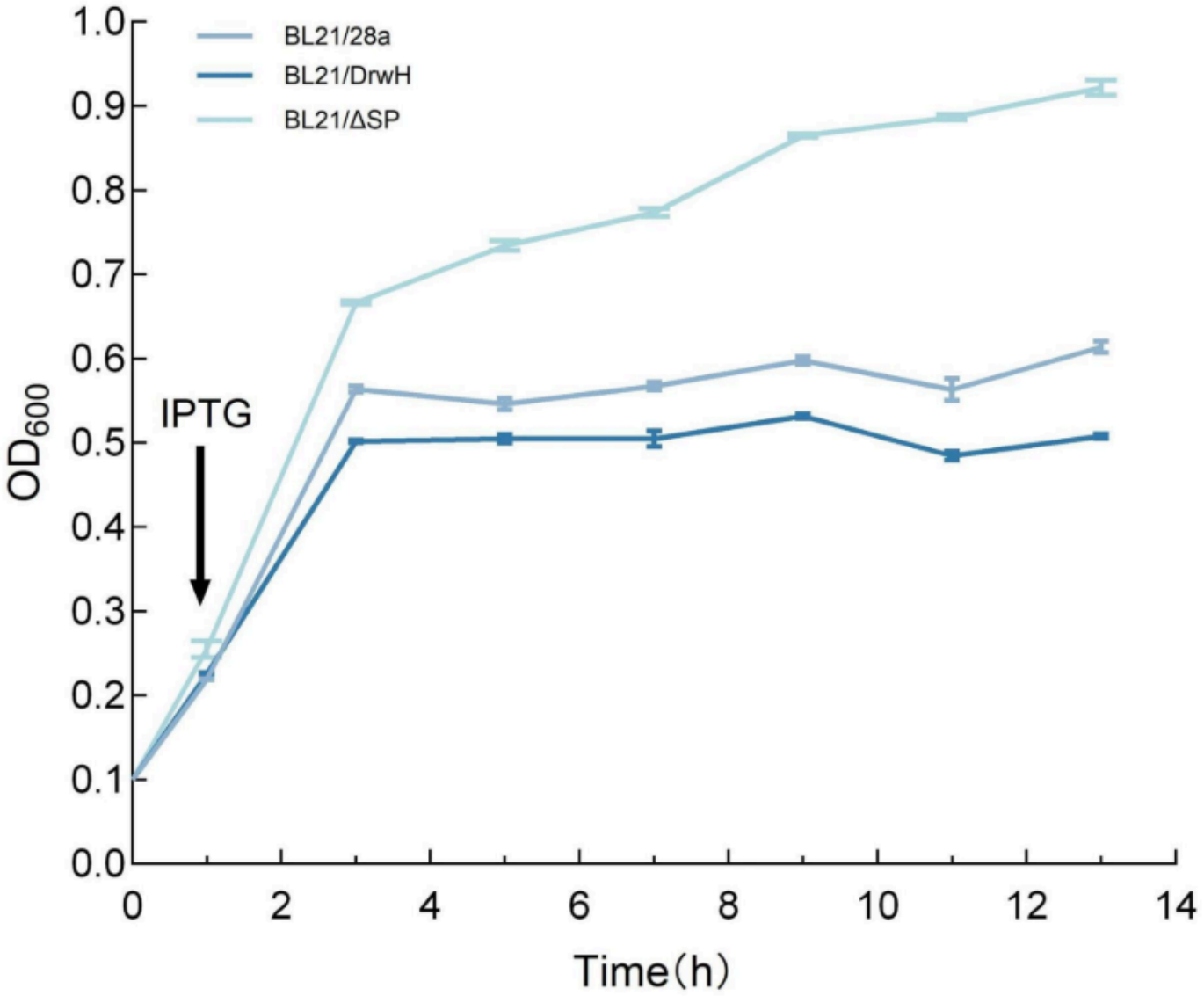


Figure 3

Growth curves of different *E. coli* strains. Protein expression was induced by adding 0.1 mM IPTG after 1 h of incubation. OD_{600} values were measured at the indicated time points to monitor the growth of BL21/28a, BL21/DrwH and BL21/ΔSP. Experiments were performed in triplicate, and data are shown as mean ± SD. One-way ANOVA followed by Tukey's test was used for statistical analysis ($P < 0.05$).

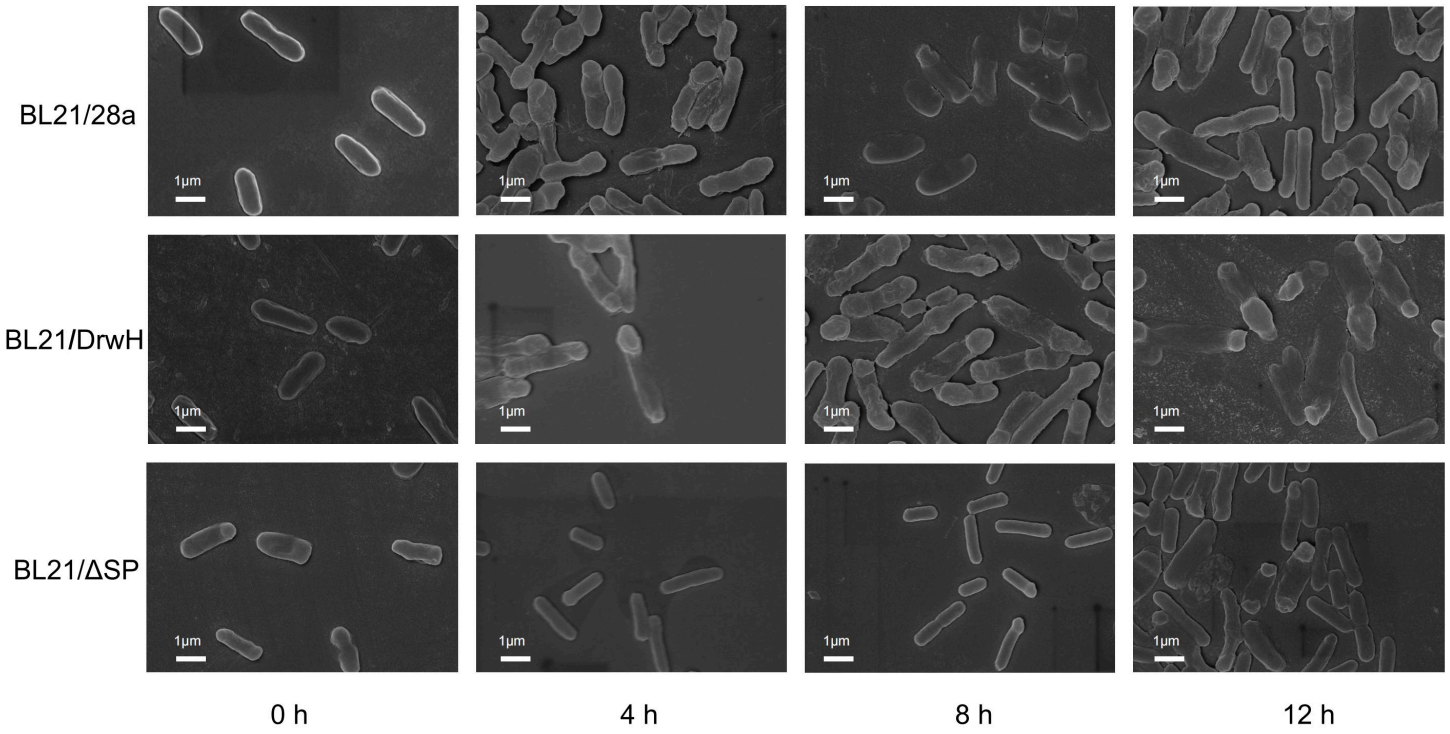


Figure 4

SEM analysis of *E. coli* strains at different time points after IPTG induction. BL21/28a, BL21/DrwH and BL21/ΔSP were harvested at 0, 4, 8 and 12 h post-induction for SEM morphological observation. Panels from left to right represent samples collected at 0, 4, 8 and 12 h, respectively. Scale bar, 1 μm.

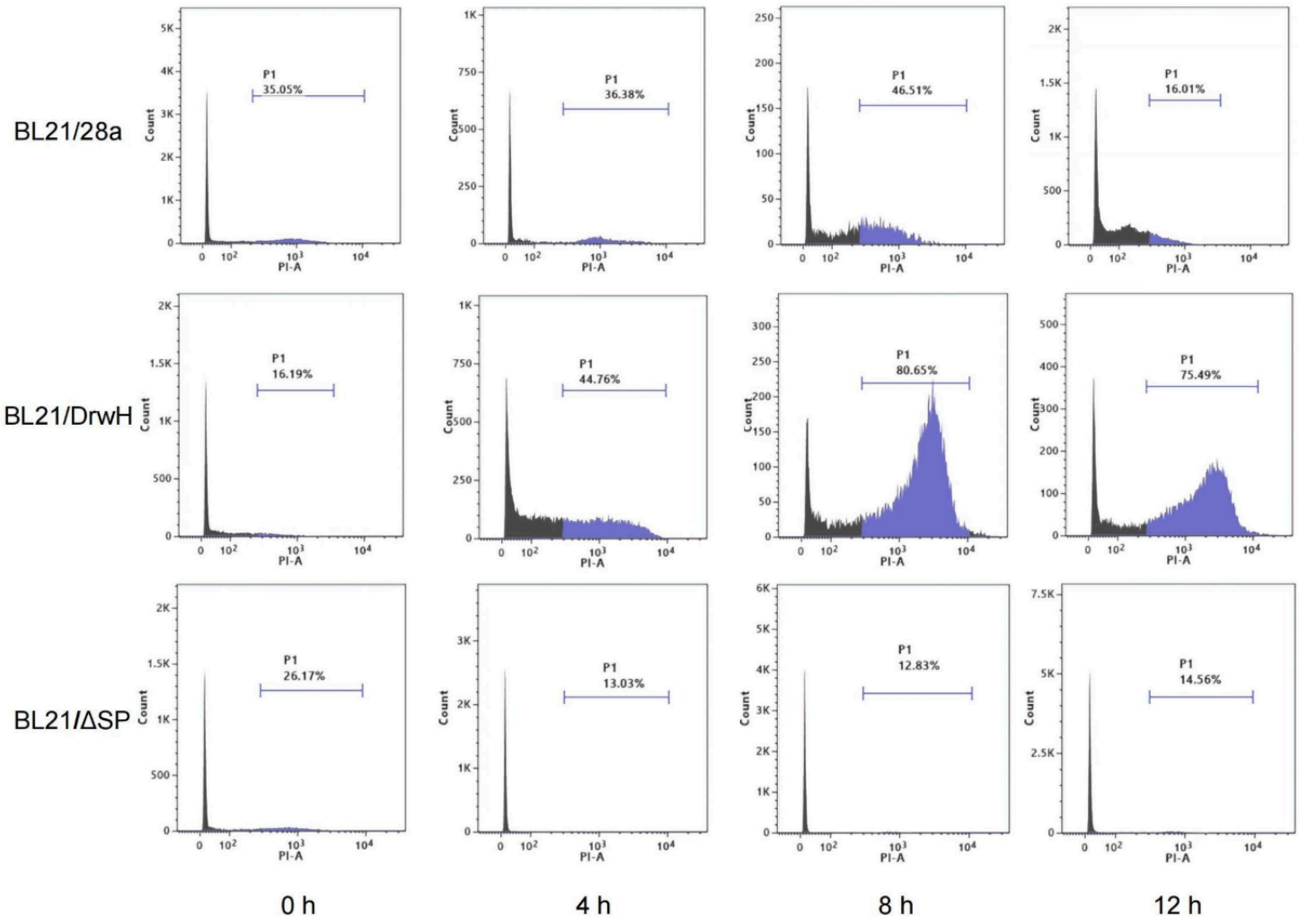


Figure 5

Flow cytometric analysis of cytotoxicity in different recombinant strains. Strains BL21/28a, BL21/DrwH and BL21/ΔSP were harvested at 0, 4, 8, and 12 h post-IPTG induction. Cell membrane permeability was assessed by flow cytometry with PI staining. Panels correspond to samples collected at 0, 4, 8 and 12 h (left to right). The P1 gate denotes the fraction of PI-positive cells. Experiments were performed in triplicate.

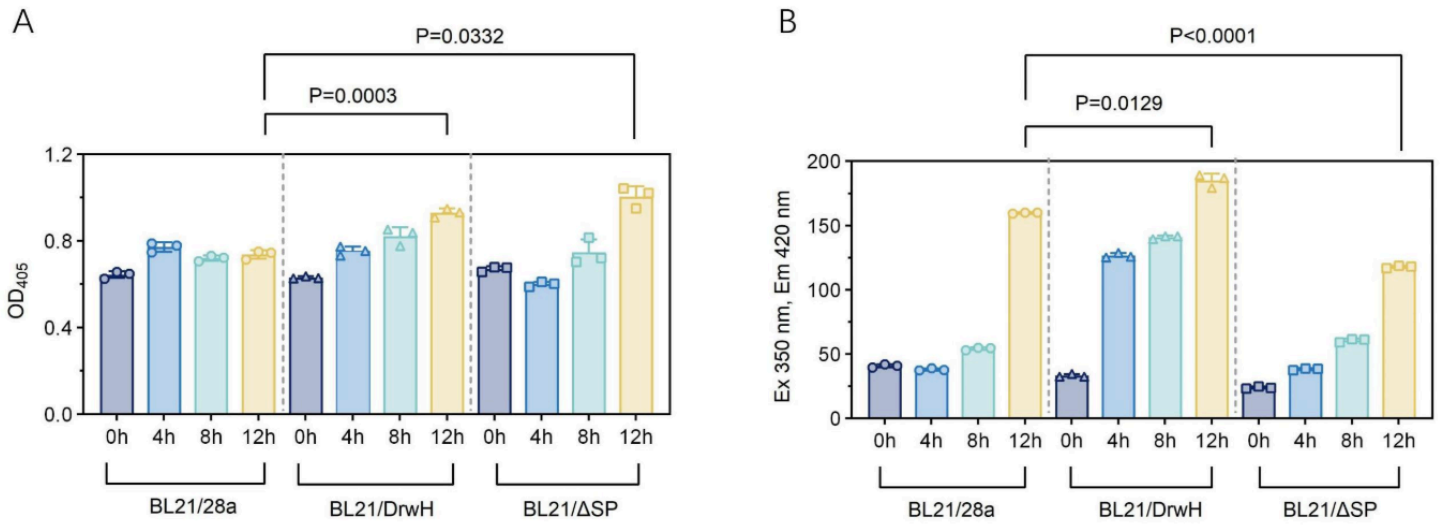


Figure 6

Quantification of outer and inner membrane permeability of *E. coli* strains at different time points after IPTG induction. Strains BL21/28a, BL21/DrwH and BL21/ΔSP were harvested at 0, 4, 8, and 12 h post-IPTG induction. (**A**) NPN fluorescence intensity (Ex 350 nm, Em 429 nm) reflects outer membrane permeability. (**B**) OD_{405} values represent inner membrane permeability determined by the ONPG assay. Data are presented as mean±SD from three independent biological replicates. Statistical significance was analysed by one-way ANOVA followed by Tukey's test.

Supplementary Files

This is a list of supplementary files associated with this preprint. Click to download.

- SPDrwHSupplementaryInformation20261014.docx